Electronic Supplementary Material

New highly soluble triarylamine-based materials as promising catholytes for redox flow batteries

Elena I. Romadina[a,b,*], Ivan A. Volodin[a], Keith J. Stevenson[a], and Pavel A. Troshin[b]

[a] Center for Energy Science and Technology, Skolkovo Institute of Science and Technology, Bolshoy Boulevard 30, bld. 1, Moscow, 143026, Russian Federation

[b] Institute for Problems of Chemical Physics, Russian Academy of Sciences, Semenov Prospect 1, Chernogolovka, Moscow region, 142432, Russian Federation

* Corresponding author *E-mail address*: Elena.romadina@skoltech.ru

Contents

1. Physico-chemical properties of triarylamine-based molecules 2
2. Experimental methods 2
2.1 Synthetic part 2
2.2 Cyclic voltammetry 2
2.3 Rotating disk electrode measurements 2
2.4 Redox flow battery tests 3
2.5 Membrane preparation 3
2.6 Solutions resistance measurements 3
2.7 Solutions pH measurements 3
Synthesis of the active compounds 4
3.1 Compound (1) {2-[2-(2-Methoxyethoxy)ethoxy]ethyl}-4-methylbenzene-sulfonate 4
3.2 Compound (2) 1-bromo-4-(2-(2-methoxyethoxy)ethoxy)benzene 4
3.3 Compound (M1) 4
3.4 Compound (M2) 5
3.5 Compound (M3) 5
3.6 Compound (M4) 5
3.7 Compound (M5) 5
3.8 Compound (M6) 5
3.9 Compound (M7) 6
3.10 Compound (V1) 1,1'-dibutyl-[4,4'-bipyridine]-1,1'-diium perchlorate 6
3. Calibration of $Ag/AgNO_3$ electrode 6
4. Multiple cyclic voltammetry tests 7
5. CV tests at -2.0 V to +1.0 V voltage range 8
6. CV tests with different concentrations of water intentionally added to the solvent 9
7. Rotation disk electrode measurements 10
8. Selection of the supporting electrolyte salt 11
9. RFB tests 12
10. RFB self-discharge experiment 14
11. Charge-discharge performance of the RFB at different current densities 15
12. Solution resistance measurements 16
13. References 17

1. Physico-chemical properties of triarylamine-based molecules

Table S1 Redox potentials, stability according to cyclic voltammetry tests, and solubility of triarylamine-based molecules.

Compound	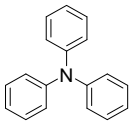	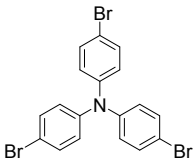	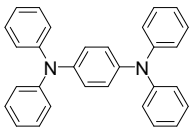	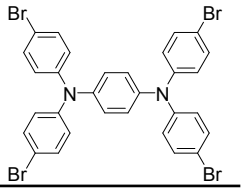
$E_{1/2}$ vs. $Ag/AgNO_3$	~0.55 V [1]	0.8 V [2]	0.18 V 0.60 V [3]	-
Solubility in MeCN	77mM *	13 mM *	0.6 mM *	Insoluble *
Reversibility of the redox process	Irreversible [1]	Reversible [2]	-	-
Cycling stability	Unstable [1]	Stable [2]	-	-

* This work

2. Experimental methods

2.1 Synthetic part

All solvents and reagents were purchased from Sigma-Aldrich or Acros Organics and used as received or purified according to standard procedures. Acetonitrile has additionally dried over 4Å molecular sieves in argon glovebox to 20 ppm water content.

The obtained compounds were purified using a preparative Shodex gel permeation chromatography (GPC) column (20 mm × 300 mm, Shodex, Japan) and toluene as eluent with the flow rate of 1 mL min^{-1}.

The purity of the all synthesized components was controlled by high-performance liquid chromatography on Shimadzu-20A instrument with the use of Orbit 100 C_{18} (5 µm, 250 × 4.6 mm, MZ-Analyentechnik GmbH, Germany) analytical column. Analyzed samples were prepared by dissolving a sample of a substance weighing 1 mg in 1 ml of a solvent used as an eluent (acetonitrile, water, or mixtures thereof).

The ^1H and ^{13}C NMR spectra were obtained using Bruker AVANCE III 500 instrument.

2.2 Cyclic voltammetry

Cyclic voltammograms were recorded in three-electrode cell with glassy carbon working electrode (WE) (d = 5 mm), $Ag/AgNO_3$ reference electrode (RE) (Basi, 10 mM $AgNO_3$ in MeCN) calibrated by ferrocene (Figure S3) and Pt wire counter electrode (CE) under argon atmosphere. Before the measurements, argon was purged through the electrolyte for 15 minutes in order to get rid of oxygen. WE was preliminarily polished with ¼ μm diamond suspension. Concentrations of the active substances were 3 mM in 0.1 M $TBABF_4$ (tetrabutylammonium tetrafluoroborate) background electrolyte based on MeCN. Measurements were performed at 0.2 V s^{-1} sweep rate on Metrohm Autolab potentiostat.

2.3 Rotating disk electrode measurements

Rotating disk electrode (RDE) measurements were performed using 1.25 mM active substance and 0.25 M supporting electrolyte ($LiPF_6$) concentrations based on anhydrous MeCN. Glassy carbon WE (d = 5 mm) was rotated by Metrohm rotor (Metrohm Autolab) in a gas-tight cell; RE – $Ag/AgNO_3$; CE – high surface glassy carbon plate; WE was preliminary polished with ¼ μm diamond suspension. Argon was purged through the electrolyte for 30 minutes before and was passed above the liquid interface during the experiment. Current-potential curves were recorded at a linear potential sweep with rotation speed varied from 300 to 2100 rpm, after the end of data recording one more IE curve was measured at 300 rpm rotation rate and compared with the first curve. Before each experiment, the impedance of the cell was measured in order to estimate working

cell resistance and to subtract ohmic drop from the experimental data. The diffusion coefficient was calculated according to Levich equation for RDE:

$I_L = 0.620 \times n \times F \times A \times D^{2/3} \times \omega^{1/2} \times v^{-1/6} \times C$

where I_L is the limiting current (A), n is the number of transferred electrons, F is the Faraday constant (C mol^{-1}), A is the electrode area (cm^2), D is the diffusion coefficient (cm^2 s^{-1}), ω is the angular rotation rate of the electrode (rad s^{-1}), v is the kinematic viscosity (cm^2 s^{-1}), C is the redox-active material concentration (mol cm^{-3}).

2.4 Redox flow battery tests

A small volume custom-made redox flow cell was used for experiments. Electrodes were cut from 6 mm thick graphite felt, and put into the assembled flow cell, providing a geometric active area of 4.00 cm^2. Anion-exchange Neosepta AHA membrane (Astom corp) was used as the separator. Teflon gaskets sealed the separator and electrodes into the cells. Flow cells were assembled inside the glovebox, where all the measurements were carried out. Peristaltic pumps (Heildolf Hei-Flow Precision 0.1 Multi or Masterflex L/S Digital Miniflex Pump) were used to drive the redox electrolytes from the reservoirs to the flow cell with the 10 mL min^{-1} flow rate.

In order to neglect crossover-provided capacity fade, the mixed electrolytes with 10 mM concentration of both active substances (catholyte and anolyte) and 0.1 M of supporting electrolyte in anhydrous MeCN were used. The volumes of electrolytes were 10 mL at each side. Combined galvanostatic and potentiostatic cycling regime was performed using Ellins potentiostate (Electrochemical instruments, Russia). Unless otherwise stated, cell was charged at 2 mA current (0.5 mA cm^{-2}) till the upper cutoff, then discharged at the same current, after reaching the lower cutoff the potential was held low for 1000 - 3000 seconds in order to provide deeper discharge of the battery, then the cycle was repeated 50 times. The theoretical capacity of the battery was 268 mA h L^{-1}.

2.5 Membrane preparation

Neosepta AHA anion exchange membrane before use was dried in vacuum at 60˚C for 24 h, conditioned in MeCN / H_2O (50:50) solvents mixture for 1h at 60˚C, in pure MeCN at 60˚C for 1 h and in 0.05 M supporting electrolyte solution in MeCN for 24 h under the room temperature and ambient conditions.

2.6 Solutions resistance measurements

Impedance curves were recorded on Metrohm Autolab potentiostat. For the measurements, the h-cell with two glassy carbon working electrodes (d = 5 mm) and two golden reference electrodes were used. Working electrodes were preliminarily polished with ¼ μm diamond suspension. Concentrations of the supporting electrolytes were 0.1 M in anhydrous MeCN; the solutions were prepared under the argon atmosphere inside the glovebox.

2.7 Solutions pH measurements

Measurements of the pH of the different electrolyte solutions with the 0.1 M supporting salts concentration were performed using portable pH/mV/˚C meter HI 83141 and pH electrode HI 1230D by HANNA instruments (USA). Solutions were prepared in anhydrous MeCN under the argon atmosphere inside the glovebox.

Table S2 pH values of different electrolytes.

Supporting electrolyte	**Pure MeCN**	**$LiPF_6$**	**$LiClO_4$**	**$TBABF_4$**	**$NaClO_4$**	**$TBAPF_6$**
pH	7.6	3.4	4.5	7.5	6.7	6.4

$TBABF_4$ = tetrabutylammonium tetrafluoroborate, $TBAPF_6$ = tetrabutylammonium hexafluorophosphate

Synthesis of the active compounds

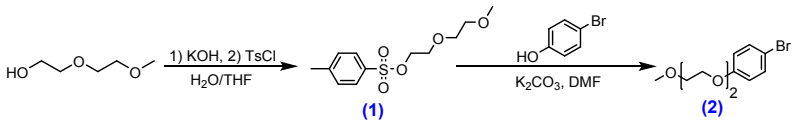

Figure S1. Synthesis of the 1-bromo-4-(2-(2-methoxyethoxy)ethoxy)benzene **(2)**

3.1 Compound (1) {2-[2-(2-Methoxyethoxy)ethoxy]ethyl}-4-methylbenzene-sulfonate

OEG-substituted tosylate **(1)** was synthesized following to the previously reported procedures [4,5] (Figure S1). Briefly, KOH (21.0 g, 0.375 mol) was dissolved in THF (60 mL) and distilled water (80 mL). 2-(2-methoxyethoxy)ethan-1-ol (30.0 g, 0.25 mol) used as starting compound dissolved in 60 ml of THF and added dropwise to KOH solutions. The reaction mixture was cooled to 0°C and *p*-toluenesulfonyl chloride (47.66 g, 0.25 mol) dissolved in THF (60 mL) was added dropwise to the mixture. After 3h, the organic compounds were extracted by CH_2Cl_2 and the resulting solution was washed with brine, dried over $MgSO_4$, and evaporated to yield 56.2 g (82%) of the target product **(1)**.

^{1}H NMR (500 MHz, $CDCl_3$): δ (ppm) 7.74 (d, 2H), 7.29 (d, 2H) 4.12 (t, 2H), 3.64 (t, 2H), 3.52 (m, 2H), 3.43 (m, 2H), 2.29 (s, 3H).

3.2 Compound (2) 1-bromo-4-(2-(2-methoxyethoxy)ethoxy)benzene

Compound **(2)** was synthesized following the previously reported procedure [6]. Bromophenol (5.60 g, 32.0 mmol), K_2CO_3 (9.00 g, 64.0 mmol) and {2-[2-(2-methoxyethoxy)ethoxy]ethyl}-4-methylbenzene-sulfonate (10.0 g, 36 mmol) were dissolved in dry dimethylformamide (DMF) (30 mL) and heated at 80˚C under Ar atmosphere for 4 h under the HPLC control. When the reaction was complete, the DMF was evaporated, the product was extracted by CH_2Cl_2, washed with water (30 mL), the organic phase was separated, dried over anhydrous Na_2SO_4 and concentrated under reduced pressure. The pure product was obtained as a light-yellow liquid (7.90 g, 92%).

^{1}H NMR (500 MHz; $CDCl_3$): δ (ppm) 7.31 (d, 2H), 6.75 (d, 2H) 4.05 (t, 2H), 3.80 (t, 2H), 3.66 (m, 2H), 3.52 (m, 2H), 3.34 (s, 3H).

^{13}C NMR (126 MHz; $CDCl_3$): 157.94, 132.23, 116.47, 71.96, 70.80, 69.69, 67.67, 59.10.

Compounds **M1**, **M2**, **M5**, and **M7** were synthesized by Buchwald–Hartwig amination reaction.

3.3 Compound (M1)

Diphenylamine (0.61 g, 3.63 mmol), 1-bromo-4-(2-(2-methoxyethoxy)ethoxy)benzene (1.00 g, 3.63 mmol), bis(dibenzylideneacetone)palladium(0) (30 mg, 0.17 mmol), sodium *tert*-butoxide (0.51 g, 4.53 mmol), tributylphosphine (14 mg, 0.7 mmol) and 60 mL of toluene were placed into a Schlenk flask charged with a reflux condenser. The reaction mixture was purged with argon for 15 min under intense stirring and then heated at reflux for 5 h under the HPLC control. After the reaction was completed, the resulting mixture was cooled down and washed with ice water (30 mL). The organic phase was separated, dried over anhydrous Na_2SO_4 and concentrated under reduced pressure. The pure product was obtained after the GPC purification as a dark-yellow viscous liquid (0.188 g, 85%).

^{1}H NMR (500 MHz; $CDCl_3$): δ (ppm) 7.25 (m, 2H), 7.19 (m, 4H), 7.05 (m, 4H), 6.92 (d, 2H), 6.84 (d, 2H), 4.11 (t, 2H), 3.85 (t, 2H), 3.71 (m, 2H), 3.57 (m, 2H), 3.38 (s, 3H). (NMR spectrum correlates with literature data [5])

^{13}C NMR (126 MHz; $CDCl_3$): δ (ppm) 155.35, 148.18, 140.98, 129.09, 127.20, 122.95, 121.88, 115.54, 72.02, 70.79, 69.85, 67.70, 59.13.

3.4 Compound (M2)

Compound **M2** was synthesized using the same procedure as described above for **M1**. Aniline (2.0 g, 21.5 mmol), 1-bromo-4-(2-(2-methoxyethoxy)ethoxy)benzene (11.83 g, 43.0 mmol), bis(dibenzylideneacetone)palladium(0) (30 mg, 0.17 mmol), sodium *tert*-butoxide (7.23 g, 64.5 mmol), tributylphosphine (14 mg, 0.7 mmol) and 100 mL of toluene were used. **M2** was obtained with 86% yield (8.68 g).

^{1}H NMR (500 MHz; $CDCl_3$): δ (ppm) 7.23 (m, 1H), 7.15 (m, 2H), 6.99 (d, 4H), 6.91 (m, 2H), 6.80 (d, 4H), 4.09 (t, 4H), 3.83 (m, 4H), 3.70 (m, 4H), 3.56 (m, 4H), 3.37 (s, 6H).

^{13}C NMR (126 MHz; $CDCl_3$): δ (ppm) 154.86, 148.73, 141.36, 128.93, 126.27, 121.13, 120.68, 115.44, 70.01, 70.77, 69.85, 67.74, 59.12.

3.5 Compound (M3)

M1 (0.20 g, 0.55 mmol) was dissolved in DMF (30 ml); *N*-Bromosuccinimide (NBS) (195 mg, 1.09 mmol) was divided into 5 parts and added to the **M1** solution gradually under intense stirring. Then, the reaction mixture was stirred at room temperature for 1 h, washed with $NaHCO_3$ aqueous solution, organic phase was separated, dried over anhydrous Na_2SO_4 and concentrated under reduced pressure. The obtained crude product was purified by GPC. The pure **M3** was obtained as a dark-yellow viscous liquid with a 91% (261 mg) yield.

^{1}H NMR (500 MHz; $CDCl_3$): δ (ppm) 7.20 (d, 2H), 6.97 (d, 4H), 6.80 (d, 4H), 6.75 (d, 2H), 4.09 (t, 2H), 3.82 (t, 2H), 3.69 (m, 2H), 3.55 (m, 2H), 3.37 (s, 3H).

^{13}C NMR (126 MHz; $CDCl_3$): δ (ppm) 155.94, 146.61, 139.91, 132.18, 127.32, 124.34, 115.78, 114.58, 72.01, 70.80, 69.78, 67.74, 59.13.

3.6 Compound (M4)

Compound **M4** was synthesized using the same procedure as described for **M3**. Compound **M2** (0.27 g, 0.57 mmol), DMF (30 ml) and NBS (97 mg, 0.54 mmol) were used. The pure product was obtained with a 90% (0.28 g) yield.

^{1}H NMR (500 MHz; $CDCl_3$): δ (ppm) 7.25 (d, 2H), 7.02 (d, 4H), 6.85 (d, 4H), 6.80 (d, 2H), 4.14 (t, 4H), 3.88 (t, 4H), 3.75 (m, 4H), 3.61 (m, 4H), 3.42 (s, 6H).

^{13}C NMR (126 MHz; $CDCl_3$): δ (ppm) 155.23, 147.90, 140.74, 131.79, 126.46, 122.16, 115.55, 112.47, 72.00, 70.78, 69.82, 67.71, 59.12.

3.7 Compound (M5)

Compound **M5** was synthesized using the same procedure as described above for **M1**. N^1,N^4-diphenylbenzene-1,4-diamine (0.50 g, 1.92 mmol), 1-bromo-4-(2-(2-methoxyethoxy)ethoxy)benzene (1.16 g, 4.22 mmol), bis(dibenzylideneacetone)palladium(0) (30 mg, 0.17 mmol), sodium tert-butoxide (0.86 g, 7.68 mmol), tributylphosphine (14 mg, 0,7 mmol) and 100 mL of toluene were used. **M5** was obtained with 81% yield (1.01 g).

^{1}H NMR (500 MHz; $CDCl_3$): δ (ppm) 7.23 (m, 2H), 7.17 (m, 4H), 7.04 (d, 4H), 6.98 (m, 4H), 6.89 (s, 4H), 6.82 (d, 4H), 4.10 (t, 4H), 3.83 (t, 4H), 3.70 (m, 4H), 3.55 (m, 4H), 3.37 (s, 6H).

^{13}C NMR (126 MHz; $CDCl_3$): δ (ppm): 155.15, 148.39, 142.69, 141.03, 129.02, 126.83, 124.51, 122.03, 121.25, 115.54, 72.00, 70.78, 69.85, 67.70, 59.13.

3.8 Compound (M6)

Compound **M6** was synthesized using the same procedure as described above for **M3**. Compound **M5** (0.22 g, 0.34 mmol), DMF (30 ml), NBS (116 mg, 0.32 mmol) were used. The pure product was obtained with a 94% (0.26 g) yield.

^{1}H NMR (500 MHz; $CDCl_3$): δ (ppm) 7.24 (d, 8H), 7.01 (d, 8H), 6.88 (s, 4H), 6.85-6.82 (m, 16H), 4.10 (t, 4H), 3.83 (t, 4H), 3.70 (m, 4H), 3.56 (m, 4H), 3.37 (s, 6H).

^{13}C NMR (126 MHz; DMSO-d^6): δ (ppm): 156.07, 147.75, 142.54, 139.80, 132.39, 127.92, 125.27, 122.87, 116.26, 112.66, 71.79, 70.20, 69.41, 67.84, 58.58.

3.9 Compound (M7)

Compound **M7** was synthesized using the same procedure as described above for **M1**. Benzene-1,4-diamine (0.33 g, 3.05 mmol), 1-bromo-4-(2-(2-methoxyethoxy)ethoxy)benzene (3.40 g, 12.0 mmol), bis(dibenzylideneacetone)palladium(0) (30 mg, 0.17 mmol), sodium tert-butoxide (2.68 g, 24.0 mmol), tributylphosphine (14 mg, 0.7 mmol) and 100 mL of toluene were used. **M7** was obtained with 77% yield (2.05 g).

^{1}H NMR (500 MHz; $CDCl_3$): δ (ppm) 6.96 (d, 8H), 6.79 (s, 4H), 6.78 (d, 8H), 4.08 (t, 8H), 3.82 (t, 8H), 3.69 (m, 8H), 3.55 (m, 8H), 3.37 (s, 12H).

^{13}C NMR (126 MHz; DMSO-d^6): δ (ppm): 156.07, 140.51, 139.82, 132.38, 129.74, 116.25, 71.80, 70.21, 69.43, 67.82, 58.58.

3.10 Compound (V1) 1,1'-dibutyl-[4,4'-bipyridine]-1,1'-diium perchlorate

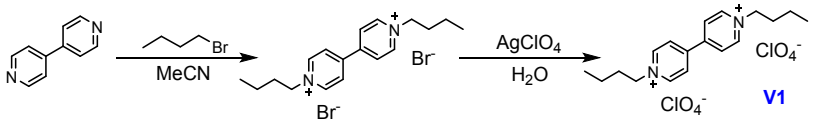

Figure S2. Synthesis of the 1,1'-dibutyl-[4,4'-bipyridine]-1,1'-diium perchlorate (**V1**)

1,1'-dibutyl-[4,4'-bipyridine]-1,1'-diium bromide was synthesized according to the previously reported procedure [7]. The ion exchange was performed by adding to the aqueous solution of 1,1'-dibutyl-[4,4'-bipyridine]-1,1'-diium bromide the equivalent amount of $AgClO_4$ in water. The precipitate of AgBr was separated by filtration, the filtrate was concentrated in vacuum and the pure product extracted from the residue by MeCN.

^{1}H NMR (500 MHz; DMSO-d^6): δ (ppm) 9.38 (d, 4H), 8.78 (d, 4H), 4.69 (t, 4H), 1.96 (quintet, 4H), 1.33 (sextet, 4H), 0.93 (t, 6H).

3. Calibration of Ag/AgNO$_3$ electrode

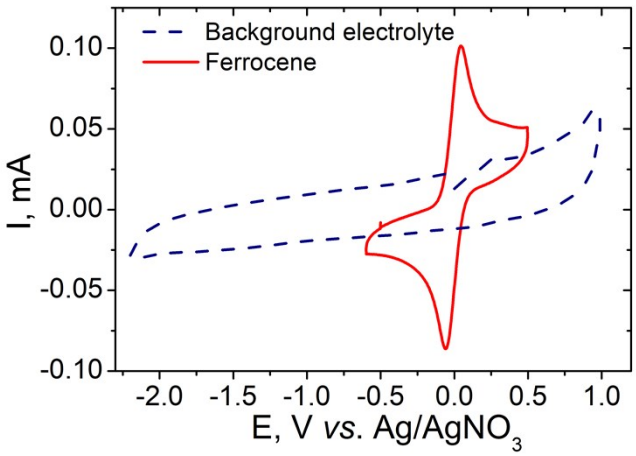

Figure S3. Cyclic voltammogram of 2.4 mM ferrocene in 0.1 M $TBABF_4$ / MeCN electrolyte.

4. *Multiple cyclic voltammetry tests*

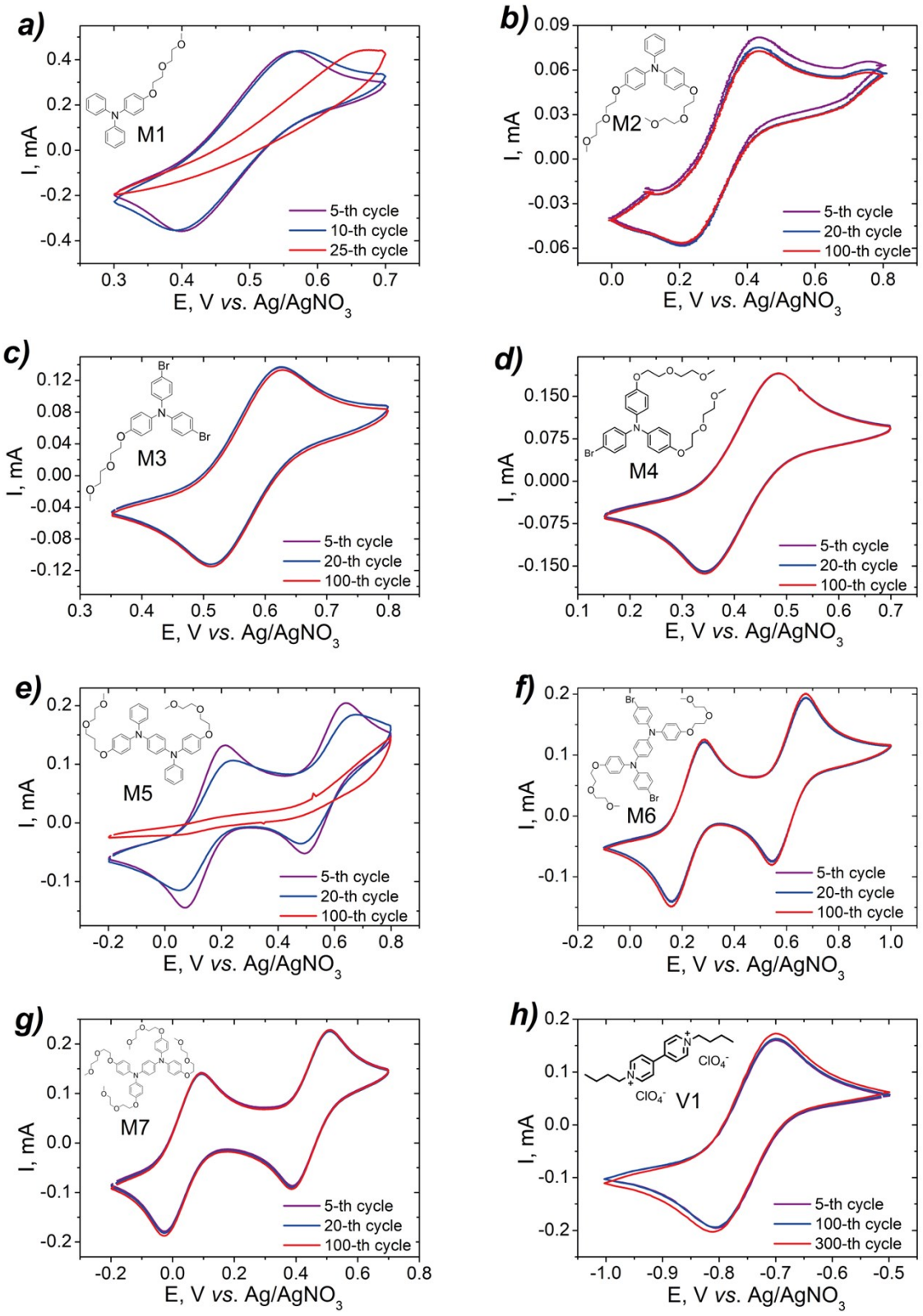

Figure S4. Cyclic voltammograms of 3 mM solutions of **M1** - **M7** (a - g) and **V1** (h) in 0.1 M $TEABF_4$ / MeCN recorded at a scan rate of 200 mV s^{-1}.

5. *CV tests at -2.0 V to +1.0 V voltage range*

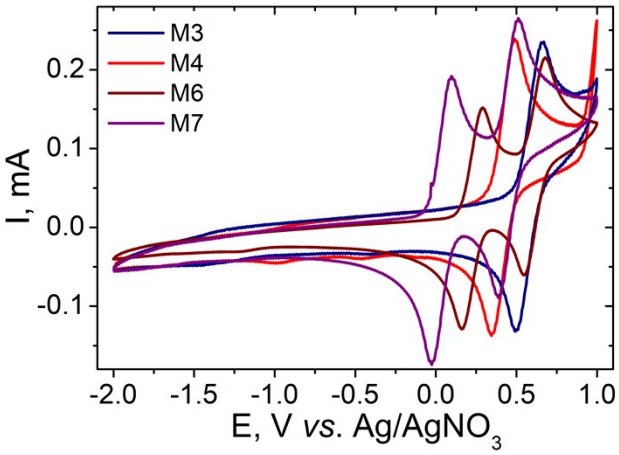

Figure S5. Cycling voltammograms obtained for 3.0 mM MeCN solution of **M3**, **M4**, **M6** and **M7** with 0.1 mol L^{-1} $TBABF_4$ as a supporting electrolyte at -2.0 V - +1.0 V voltage range.

6. *CV tests with different concentrations of water intentionally added to the solvent*

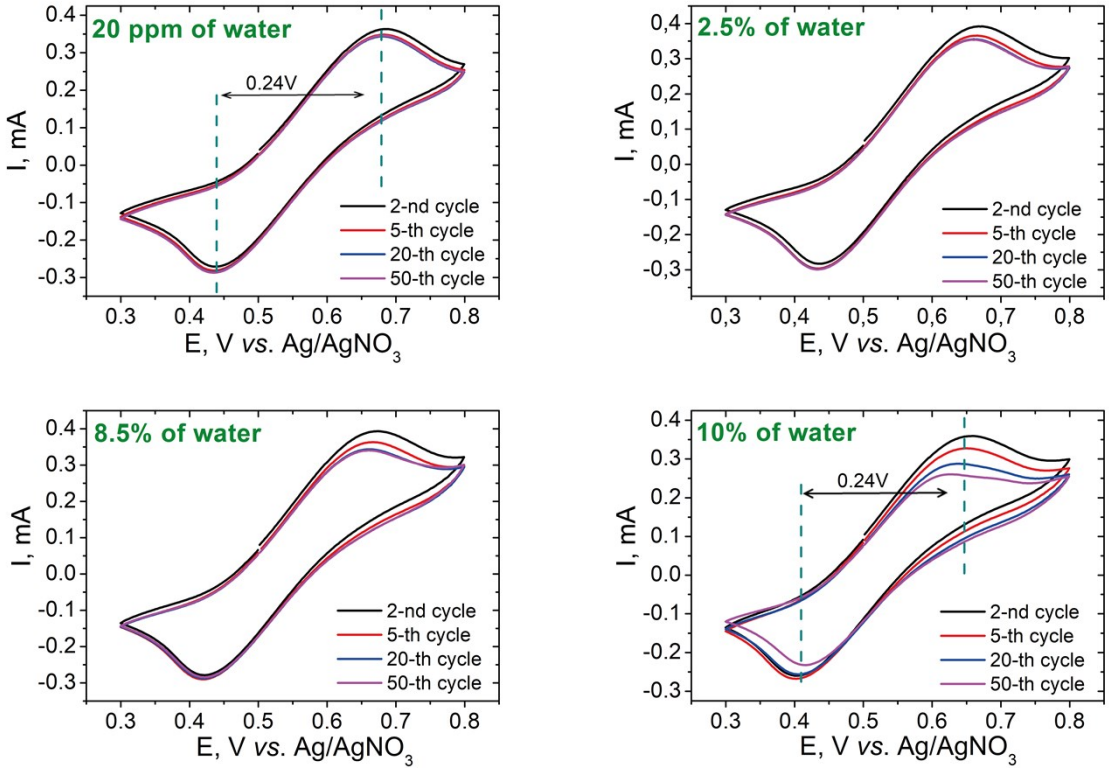

Figure S6. Cyclic voltammograms of 10 mM **M3** in 0.25 M $TBABF_4$ / MeCN at a scan rate of 200 mV s^{-1} with different amounts of water in the solvent.

7. Rotation disk electrode measurements

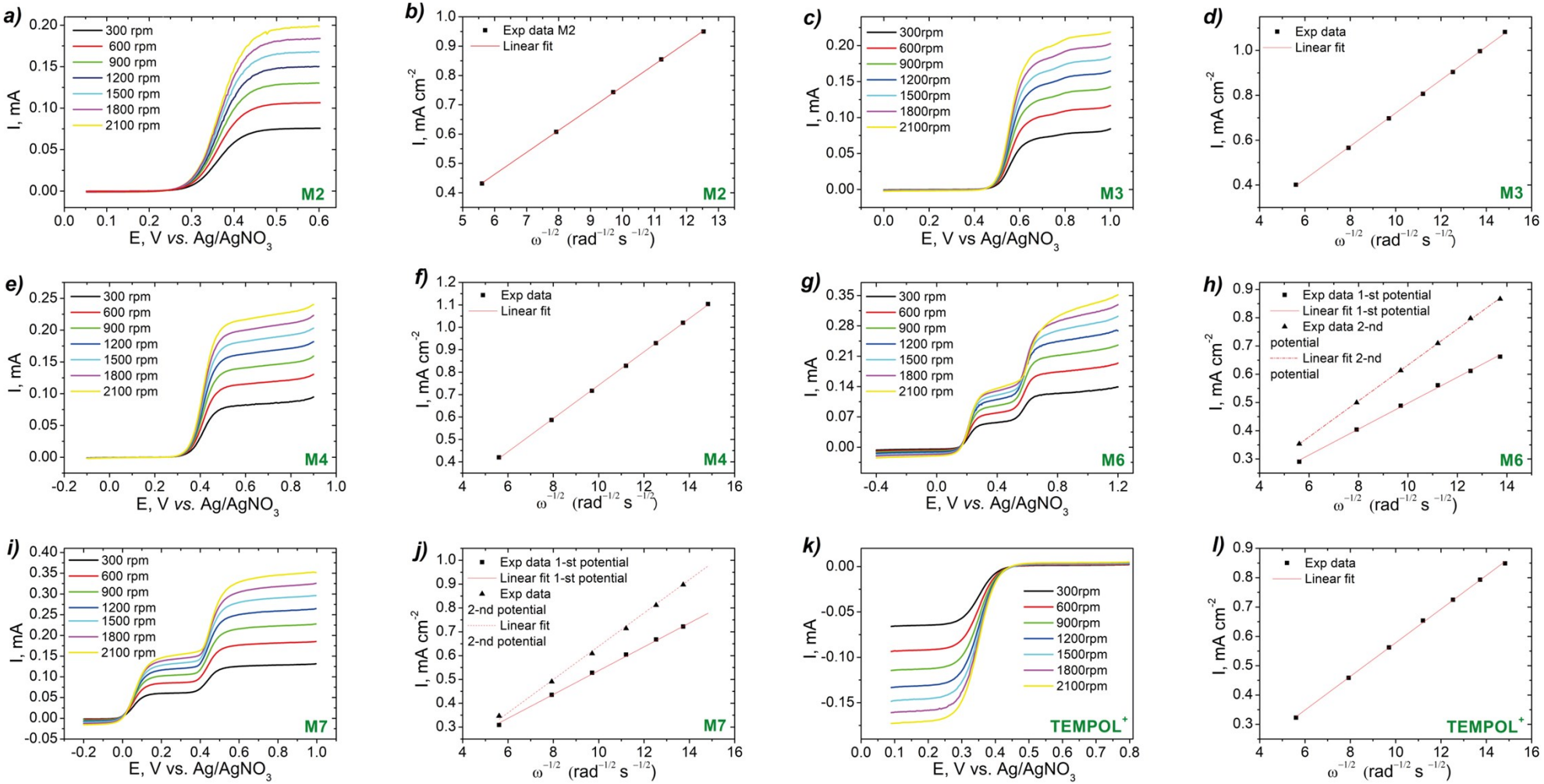

Figure S7. Linear sweep voltammetry tests with a glassy carbon rotating disk electrode for the **M2** (a), **M3** (c), **M4** (e), **M6** (g), **M7** (i), $TEMPOL^+$ (k) molecules; linear plots of the current as a function of the square root of the rotation rate (ω) for the **M2** (b), **M3** (d), **M4** (f), **M6** (h), **M7** (j) and $TEMPOL^+$ (l) molecules. Concentration of the active species was 1.25 mM, concentration of the supporting electrolyte ($LiPF_6$) was 0.25 M, anhydrous MeCN was use as a solvent.

8. Selection of the supporting electrolyte salt

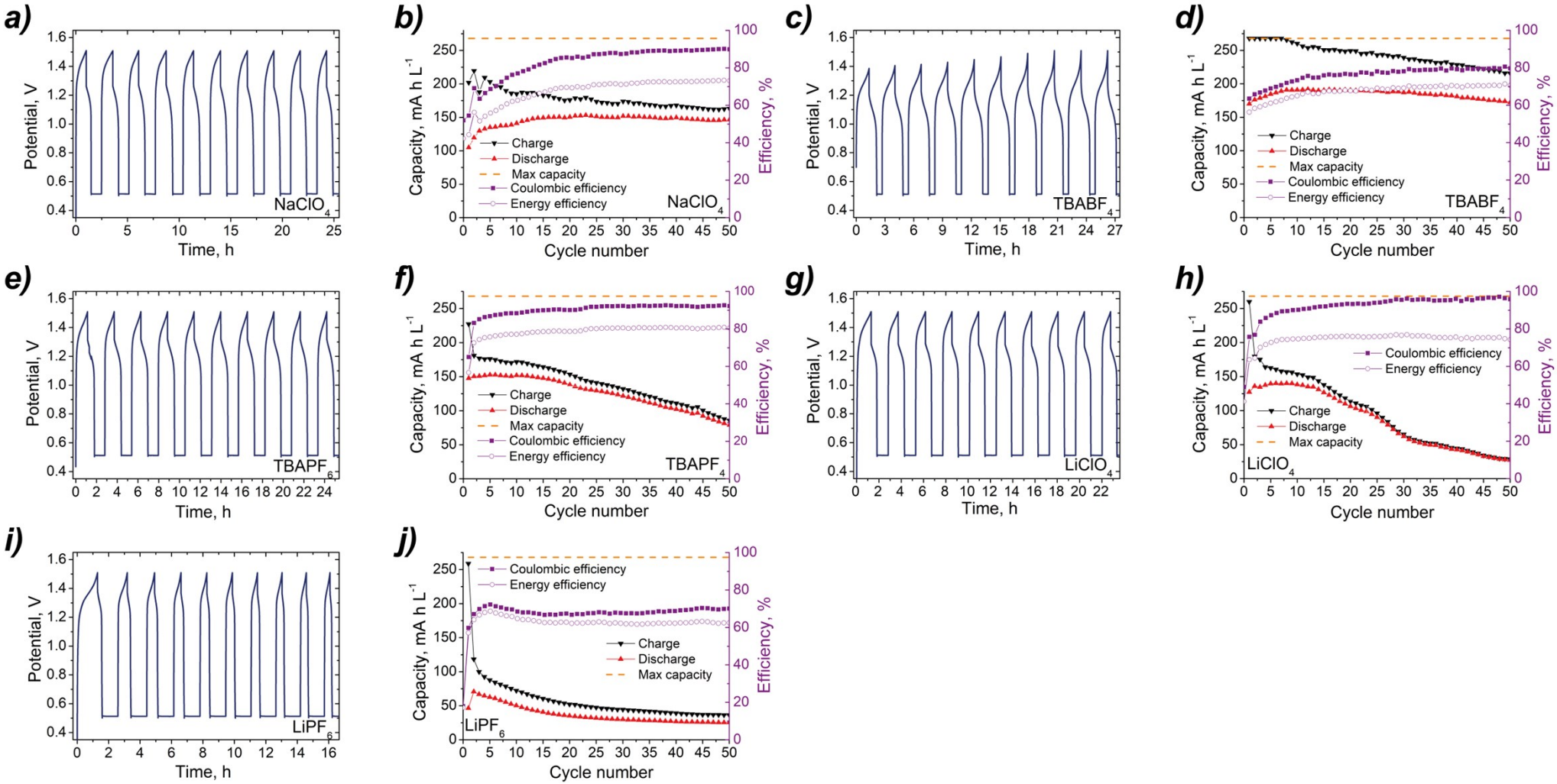

Figure S8. Potential-time dependence curves (a, c, e, g, i), charge-discharge capacities and Coulombic and Energy efficiencies (b, d, f, i) of the **M3**/**V1** redox flow cells assembled with different supporting electrolytes: $NaClO_4$ (a, b), $TBABF_4$ (c, d), $TBAPF_6$ (e, f), $LiClO_4$ (g, h), $LiPF_6$ (i, j). Conditions: mixed electrolytes with 10 mM concentration of active substances (**M3** and **V1**) and 0.1 M of supporting electrolytes in anhydrous MeCN. The theoretical capacity was 268 mA h L^{-1}. Charge-discharge current density was 0.5 mA cm^{-2}.

9. RFB tests

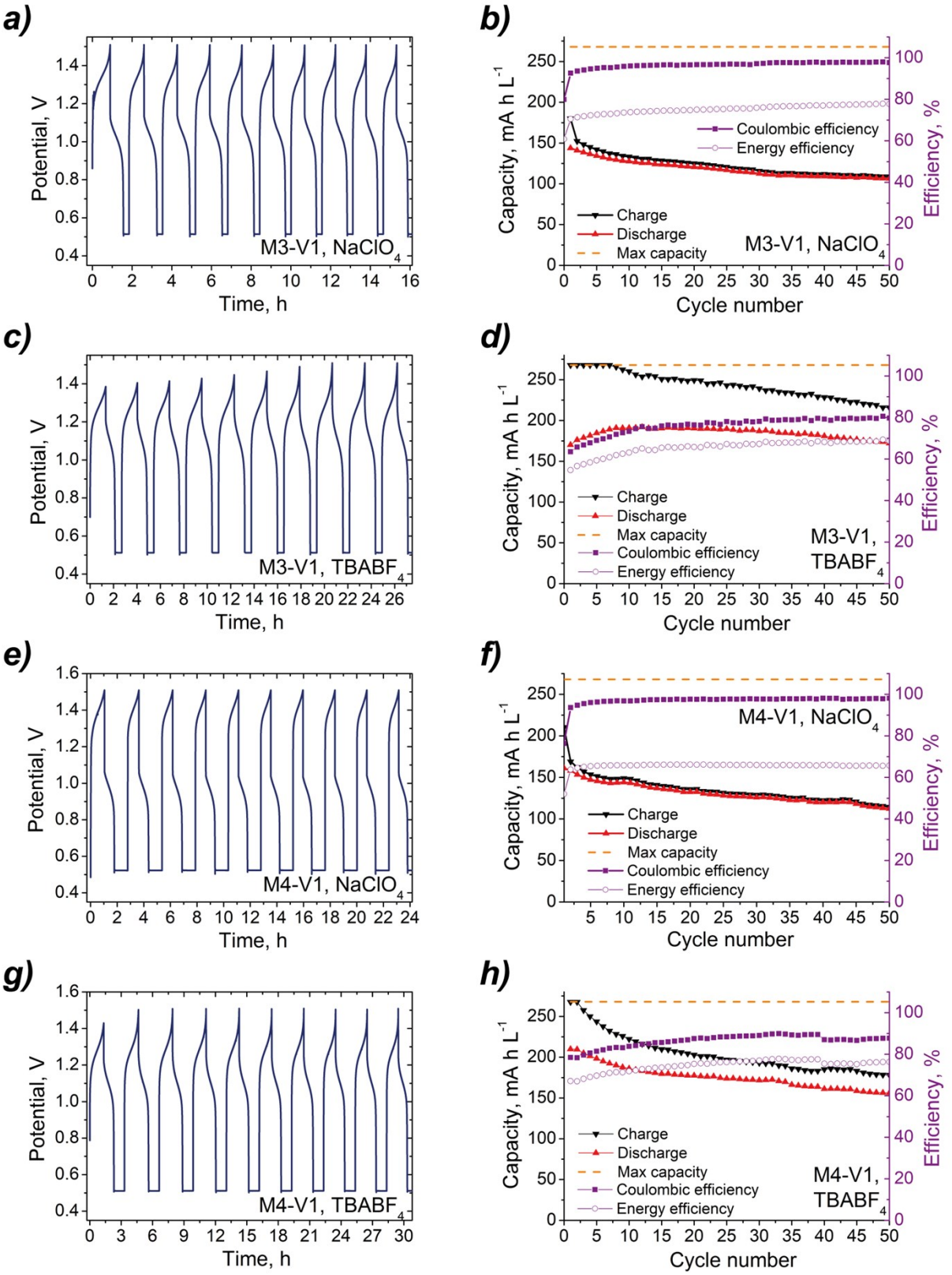

Figure S9. Electrochemical performance of the **M3/V1** (a-d) and **M4/V1** (e-h) flow cells with $NaClO_4$ (a-b, e-f) and $TBABF_4$ (c-d, g-h) supporting electrolytes: potential-time dependence curves (a, c, e, g), charge-discharge capacities and Coulombic and Energy efficiencies (b, d, f, h). Conditions: mixed electrolytes with 10 mM concentration of catholytes and anolyte and 0.1 M of supporting electrolytes in anhydrous MeCN. The theoretical capacity was 268 mA h L^{-1}. Charge-discharge current density was 0.5 mA cm^{-2}.

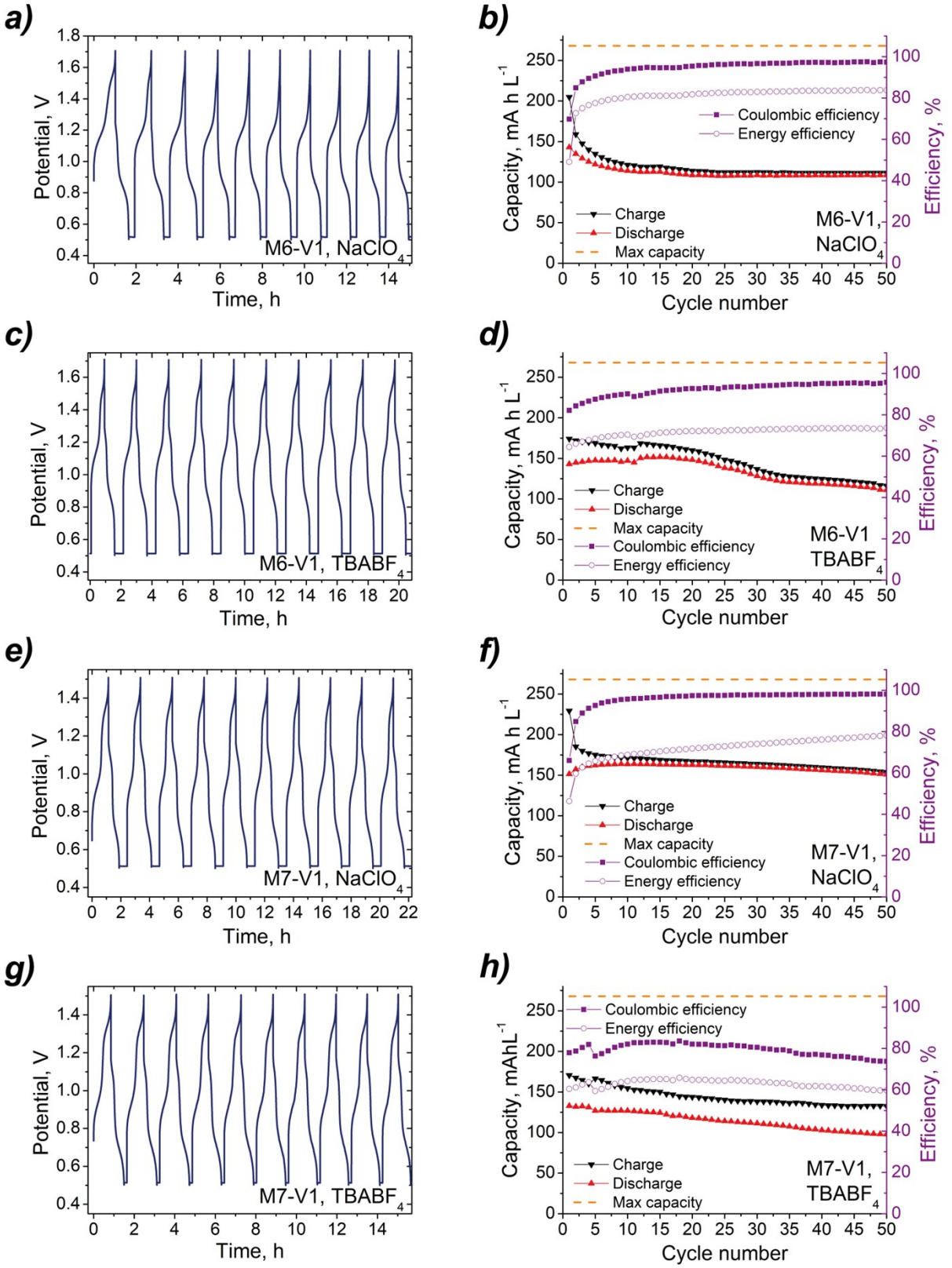

Figure S10. Electrochemical performance of the **M6/V1** (a-d) and **M7/V1** (e-h) flow cells with $NaClO_4$ (a-b, e-f) and $TBABF_4$ (c-d, g-h) supporting electrolytes: potential-time dependence curves (a, c, e, g), charge-discharge capacities and Coulombic and Energy efficiencies (b, d, f, h). Conditions: mixed electrolytes with 5 mM concentration of catholytes and 10 mM concentration of anolyte and 0.1 M of supporting electrolytes in anhydrous MeCN. The theoretical capacity was 268 mA h L^{-1}. Charge-discharge current density was 0.5 mA cm^{-2}.

10.RFB self-discharge experiment

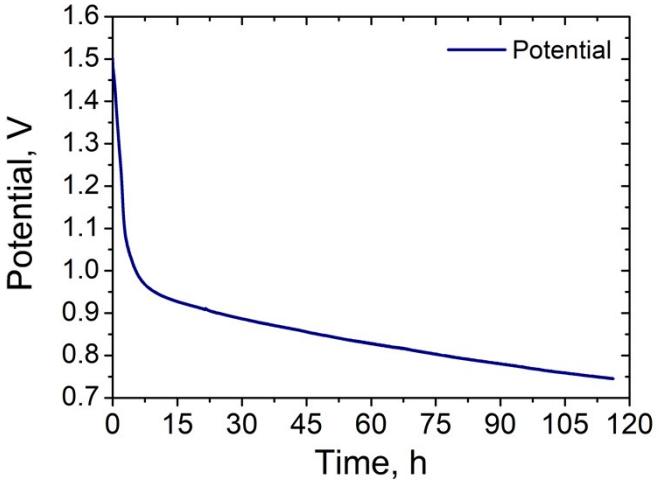

Fig. S11. Self-discharge experiment consisting of monitoring the evolution of the RFB potential over time at the flow rate of 3 ml min^{-1}.

11. Charge-discharge performance of the RFB at different current densities

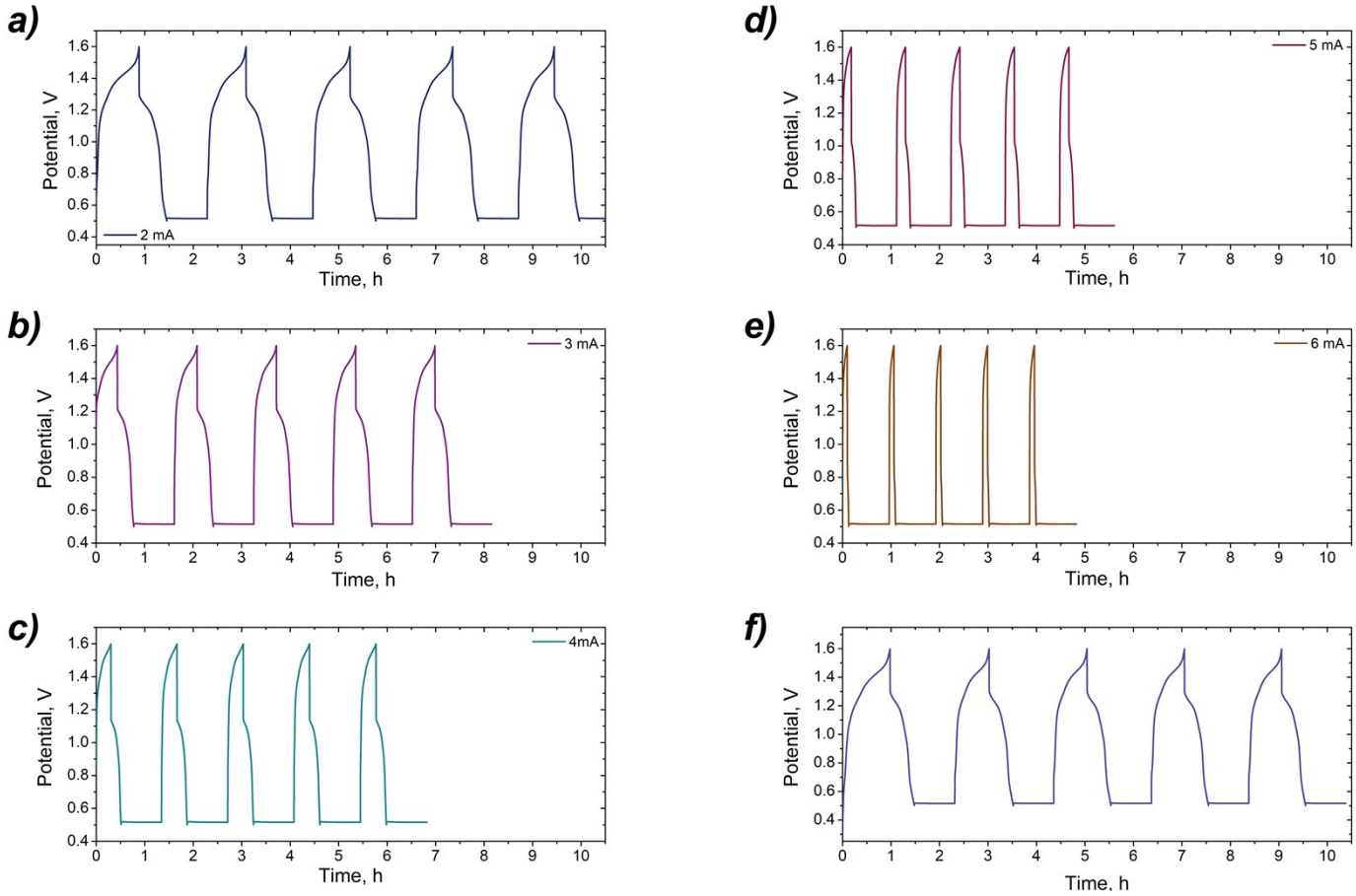

Fig. S12. Potential-time dependence curves of the **M3/V1** redox flow cell with $TBABF_4$ supporting electrolyte for the different charge-discharge currents: (a) 2 mA, (b) 3 mA, (c) 4 mA, (d) 5 mA, (e) 6 mA (f) 2 mA terminatory experiment. Conditions: mixed electrolytes with 10 mM concentration of active substances (**M3** and **V1**) and 0.1 M of supporting electrolytes in anhydrous MeCN. The theoretical capacity was 268 mA h L^{-1}.

12. *Solution resistance measurements*

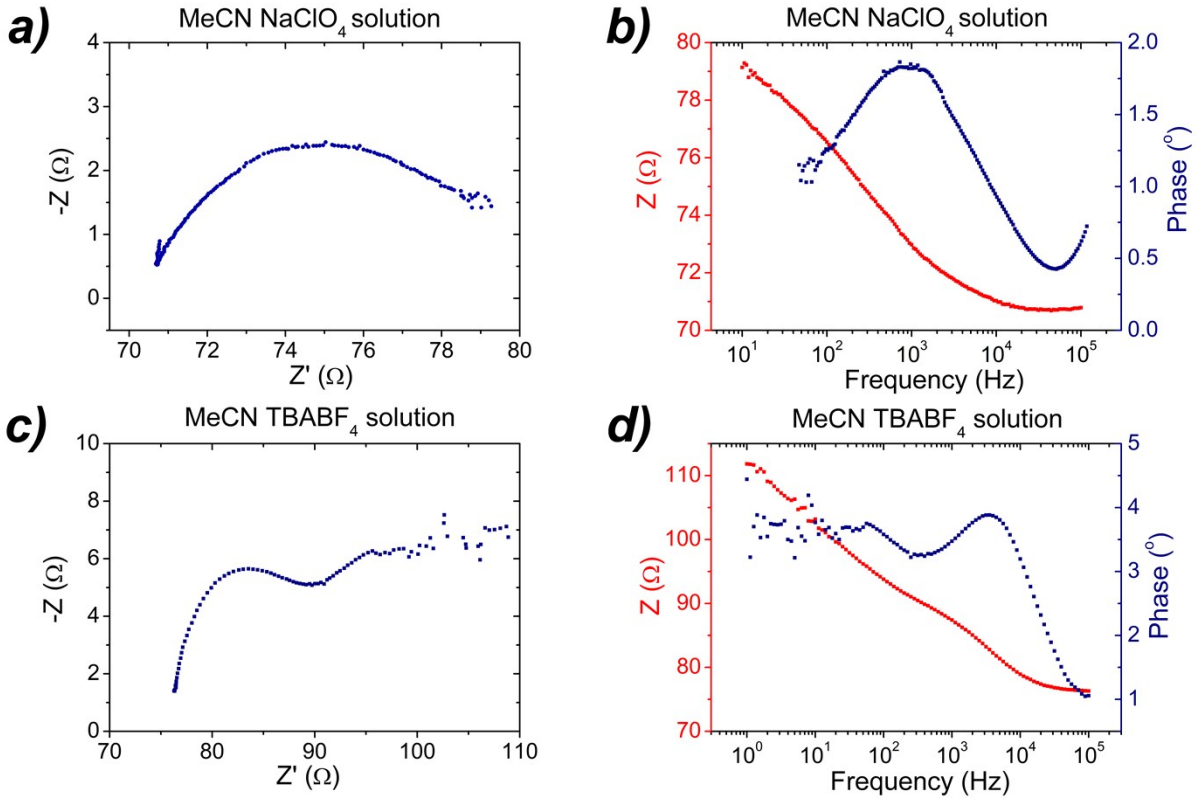

Fig. S13. (a) The Nyquist Plot of the 0.1 M $NaClO_4$ MeCN solution; (b) The Bode Plot of the 0.1 M $NaClO_4$ MeCN solution; (c) The Nyquist Plot of the 0.1 M $TBABF_4$ MeCN solution; (d) The Bode Plot of the 0.1 M $TBABF_4$ MeCN solution.

13. References

1 E. T. Seo, R. F. Nelson, J. M. Fritsch, L. S. Marcoux, D. W. Leedy and R. N. Adams, *J. Am. Chem. Soc.*, 1966, **178**, 3498–3503.

2 V. Pasala, C. Ramachandra, S. Sethuraman and K. Ramanujam, *J. Electrochem. Soc.*, 2018, **165**, A2696–A2702.

3 C. Wu, P. I. Djurovich and M. E. Thompson, *Adv. Funct. Mater.*, 2009, **19**, 3157–3164.

4 Y. Kim, J. Choi, C. Lee, Y. Kim, C. Kim, T. L. Nguyen, B. Gautam, K. Gundogdu, H. Y. Woo and B. J. Kim, *Chem. Mater.*, 2018, **30**, 5663–5672.

5 K. Willinger, K. Fischer, R. Kisselev and M. Thelakkat, *J. Mater. Chem.*, 2009, **19**, 5364–5376.

6 W. Liu, L. Liang, P. K. Lo, X. J. Gou and X. H. Sun, *Tetrahedron Lett.*, 2016, **57**, 959–963.

7 J. H. Ross and R. I. Krieger, *J. Agric. Food Chem*, 1980, **26**, 1026–1031.